Optical Materials EXPRESS

Energy transfer in iron-chromium co-doped ZnSe middle-infrared laser crystals

VLADIMIR FEDOROV,[1,2,*] **TRISTAN CARLSON,**[1] **AND SERGEY MIROV**[1,2]

[1] *Department of Physics, University of Alabama at Birmingham, CH 310, 1300 University Blvd., Birmingham, AL 35294, USA*
[2] *IPG Photonics Corporation Southeast Technology Center 100 Lucerne Lane, Birmingham, AL 35211, USA*
[*] *vfedorov@uab.edu*

Abstract: We report on the characterization of energy transfer in iron-chromium co-doped ZnSe middle-infrared laser crystals. The room temperature kinetics of the Fe:Cr:ZnSe sample under excitation of chromium ion at 1560 nm shows that energy transfer in Fe-Cr centers could be as fast as 290 ns. This rate is close to the non-radiative relaxation rate of Fe^{2+} ions in this host. The analysis of energy transfer rate in Cr-Cr; Fe-Fe and Cr-Fe pairs based on the resonance dipole-dipole interaction showed that energy transfer rate could be as fast as 10^9 s^{-1}.

1. Introduction

Iron doped chalcogenide media are attractive materials for development of tunable middle-infrared (mid-IR) solid-state lasers. The first Fe:ZnSe laser operating at T = 180 K was demonstrated in [1]. The upper laser level of Fe^{2+} ions is quenched at room temperature (RT), however, the RT gain-switched oscillation regime could be efficient, as was first reported for the Fe:ZnSe laser in [2]. Crystal field engineering allows modification of the spectral position of Fe^{2+} emission and absorption bands enabling ultra-broad (3.5-8.0 µm) tunability of a variety of Fe-doped II-VI binary, ternary, and quaternary compounds [3,4,5,6]. Arguably, the Fe:ZnSe laser is the most advanced among other iron doped chalcogenide systems. The broad absorption band of Fe^{2+} ions in ZnSe crystal is centered at 3.1µm. Several laser sources were used for the excitation of Fe^{2+} lasers including: Er:YAG@2.9 µm laser; Cr:ZnSe@2.7µm laser; D2 Raman Shifted@2.92 µm (2nd Stokes) Nd:YAG laser radiation; and HF@2.6-3.1 µm laser [7,8,9]. However, there is a strong demand for the development of laser systems with a more convenient pump source. One of the ways to overcome the limitation of available pump sources could be using an energy transfer process between different transition metals ions. Cobalt ions in II-VI semiconductors feature strong absorption bands near 0.8 µm and 1.5 µm and could be used for this application. Also, the luminescence band of Co^{2+} ions overlaps well with the absorption band of Fe^{2+} ions. Fe^{2+} laser oscillation in Co:Fe:ZnS(ZnSe) co-doped crystals was demonstrated under 0.790 µm and 1.56 µm pumping of Co^{2+} ions [10,11]. Unfortunately, laser oscillation was realized only at low temperature (<24 K) due to the overlap of the excited state absorption of Co^{2+} ions with the Fe^{2+} luminescence band at higher temperatures. The energy splitting of the Fe^{2+} ions is smaller than that of the Cr^{2+} ions. As depicted in Fig. 1, it results in the overlap of the emission band of the Cr^{2+} ions with the absorption band of Fe^{2+} ions. It also allows for Förster resonance energy transfer between chromium and iron ions. The $Cr^{2+}\rightarrow Fe^{2+}$ energy transfer in low doped crystals was demonstrated in [4]. In this paper we report on luminescence and kinetic characterization of Fe:Cr:ZnSe samples under excitation of Cr^{2+} ions. We also discuss the energy transfer rate in Cr-Cr; Fe-Fe and Cr-Fe pairs due to the resonance dipole-dipole interaction.

#357782
Journal © 2019

https://doi.org/10.1364/OME.9.002340
Received 14 Jan 2019; revised 1 Apr 2019; accepted 2 Apr 2019; published 25 Apr 2019

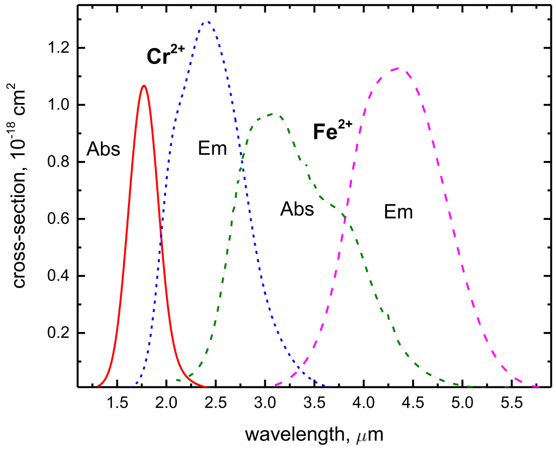

Fig. 1. Absorption and emission cross-sections of Cr^{2+} and Fe^{2+} ion at $^5T_2 \leftrightarrow {}^5E$ transition in ZnSe crystal at RT.

2. Experimental results

Polycrystalline ZnSe gain elements were utilized in this work. ZnSe undoped crystals were grown by a chemical vapor transport technique. Further, ZnSe crystal doping with Fe and Cr was accomplished in a sealed vacuum ampoule via a multi-step post growth thermal diffusion process from Fe and Cr thin films deposited on the crystal surface. After iron doping, the Fe:ZnSe sample was cut and one part of the sample was co-doped by chromium ions. In addition, the Cr:ZnSe crystal was also fabricated in the same process for comparison. Transition metal (TM) ion concentrations were calculated from the absorption measurements and absorption cross sections well documented in the literature. Figure 2 shows the absorption spectra of the fabricated crystals.

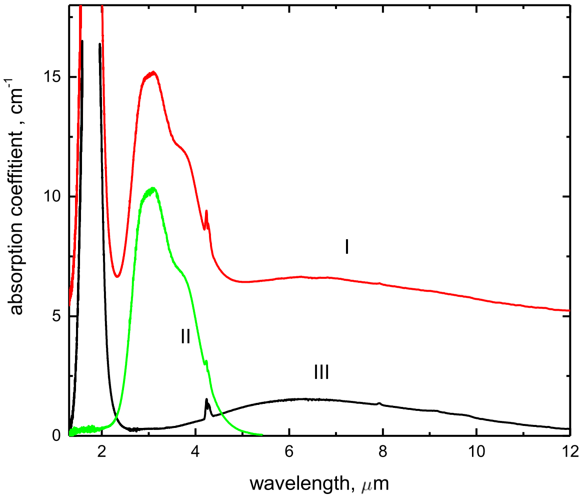

Fig. 2. (A) Absorption spectra of Fe:Cr:ZnSe (I), Fe:ZnSe(II), and Cr:ZnSe(III) samples. The spectrum of the Fe:Cr:ZnSe crystal was shifted on 5 cm^{-1} along the “y” axis for better visibility.

The spectrum of the Fe:Cr:ZnSe crystal was shifted 5 cm^{-1} along the “y” axis for better visibility. We used absorption cross-sections of 1.1×10^{-18} cm^2 at 1.77 μm for Cr^{2+} ions and

0.97×10^{-18} cm^2 at 3.1 µm for Fe^{2+} ions [12]. The absorption spectra of the Cr^{2+} and Fe^{2+} bands in the co-doped Fe:Cr:ZnSe sample were identical to the absorption bands in Fe:ZnSe and Cr:ZnSe samples doped under the same conditions. It indicates that additional co-doping does not affect the absorption cross-section for used concentrations. The chromium concertation in the Cr:ZnSe and Fe:Cr:ZnSe samples was calculated to be 2.2×10^{19} cm^{-3}. The iron concentration was equal to 1.0×10^{19} cm^{-3} in the Fe:Cr:ZnSe and Fe:ZnSe crystals.

Kinetics of Fe^{2+} luminescence in the 3500-5500 nm spectral range are shown in Fig. 3. In our experiments we used the radiation of a Q-switched Er:YAG@2.94 µm laser for direct excitation of the $^5E \rightarrow {}^5T_2$ transition. For chromium excitation, a D_2 Raman shifted Nd:YAG laser oscillation at 1560 nm was used. The detector has a temporal resolution of ~80 ns.

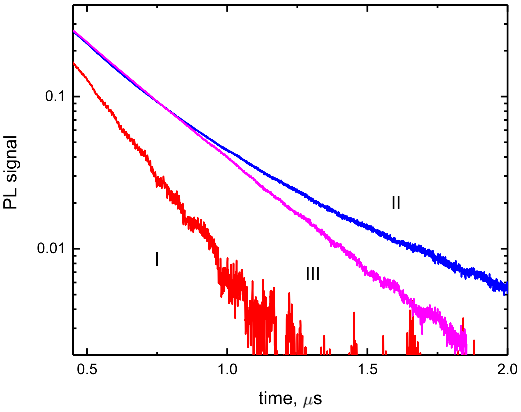

Fig. 3. RT Kinetics of Fe^{2+} ions in Fe:Cr:ZnSe (I, II) and Fe:ZnSe (III) crystals under excitation by 1560 nm (II) nm and 2940 nm (I, III) radiation.

The PL of the Cr:ZnSe sample was measured to be 5 µs under direct excitation into chromium absorption band which is smaller than radiative lifetime (5.5 µs) of the Cr^{2+} ions measured at low concentration level [12]. This data is close to the data reported earlier by [13]. In this publication authors studied concentration quenching Cr^{2+} ion photoluminescence and reported a decrease in life-time of Cr^{2+} ion photoluminescence to ~5 µs for a sample with a chromium concentration of ~2x10^{19} cm^{-3}. It should be noted, that some authors reported stronger concentration quenching of chromium photoluminescence. For example, the 2.4 µs life-time was measured for the sample with a chromium concentration of 2.6×10^{19} cm^{-3} in [14]. However, in this study, the thermal diffusion from the gas phase was carried out at temperatures below 850°C and for 6 days only. We believe that inhomogeneous distribution of the chromium ions could be responsible for stronger concentration quenching.

The Fe:ZnSe crystal has an exponential decay time with constant $\tau = 290$ ns (Fig. 3, curve III). It is smaller than that for the crystal with small iron concentration (380 ns)[15]. This indicates that the rate of Fe-Fe interaction with a concentration of ~10^{19} cm^{-3} is comparable with non-radiative relaxation at RT. Under direct excitation of Fe^{2+} ions in the Fe:Cr:ZnSe sample, the photoluminescence decay was single exponential within experimental errors. While the Fe:Cr:ZnSe crystal has the same iron concentration as the Fe:ZnSe sample, it has faster exponential decay with a ~180 ns decay time (Fig. 3, curve I). It could be due to the energy transfer from the $^5T_2$ iron level to the components of $^5T_2$ levels of Cr^{2+} ions.

The kinetics of Fe^{2+} ions in Fe:Cr:ZnSe under excitation into the chromium absorption band is also shown in the Fig. 3 (curve II). With the accuracy of detector response time, we did not observe rise-time of the iron photoluminescence due to the energy transfer process after excitation into the chromium absorption band. The kinetics is not single exponential. The rate of energy transfer depends on the donor-to-acceptor separation distance (R) (as $\sim R^{-6}$ for dipole-dipole interaction). Variation of the donor-to-acceptor distance separation results in a different rate for different ions and a non-exponential decay curve. The fastest decay rate should be for the centers where Cr and Fe ions occupy the nearest cation sites. This rate could be estimated from the beginning of the decay curve. In our Fe:ZnSe sample, the initial stage of the decay (curve II) was close to the decay of the Fe:ZnSe sample and equal to 290 ns. The kinetics constants in iron and chromium doped ZnSe crystals are summarized in Table 1.

Table 1. Summary of kinetics constants in iron and chromium doped ZnSe crystals from experimental measurements (meas.) and calculated (cal.) using Förster resonance energy transfer

Parameter		N[Fe^{2+}] x10^{19} cm^{-3}	N[Cr^{2+}] x10^{19} cm^{-3}
Fe^{2+} ion Radiative life time[a],<150 K (meas.)	55 µs	<0.1	0
Fe^{2+} ion life time, RT[a] (meas.)	380 ns	<1	0
Fe^{2+} ion life time, RT (meas.)	290 ns	1	0
Cr-Fe energy transfer kinetics, (meas.)	180 ns	1	2
Cr-Cr energy transfer, (R_{min}) (cal.)	1.4 ns	-	-
Cr-Cr energy transfer, (R_N=3.7 nm) (cal.)	850 µs	2	0
Fe-Fe energy transfer, (R_{min}) , (cal.)	0.37 ns	-	-
Fe-Fe energy transfer, (R_N=3.7 nm), (cal.)	230 µs	0	2
Cr-Fe energy transfer, (R_{min}), (cal.)	0.320 ns	-	-
Cr-Fe energy transfer, (R_N=3.7 nm), (cal.)	200 µs	1	1

[a] From IEEE Journal of Selected Topics In Quantum Electronics, 21(1) #: 1601719(2015).

We also compared the photoluminescence (PL) spectra of Cr:ZnSe and Fe:Cr:ZnSe samples in the 2-3 µm spectral range under direct excitation into the chromium band by the radiation of a CW Er-fiber laser operating at 1.56 µm (see Fig. 4). As we describe above, Cr:ZnSe and Fe:Cr:ZnSe samples had the same chromium concentration and were polished in the same process. The excitation area of the studied samples was limited by installed aperture which was smaller than sample sizes. The setup was designed so that the replacement of experimental samples was not accompanied by setup realignment. The PL signal below 2 µm was blocked by a bandpass optical filter. As one can see from the Fig. 4, the PL signal from the Cr:Fe:ZnSe co-doped sample was 6 times smaller than that of Cr:ZnSe samples with the same chromium concentration. This indicates that Cr→Fe energy transfer is faster than the upper level lifetime of the Cr^{2+} ions.

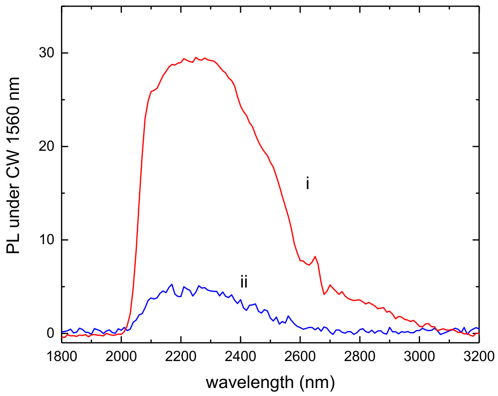

Fig. 4. Photoluminescence spectra of Cr:ZnSe (i) and Fe:Cr:ZnSe crystals under CW excitation at 1.56 µm.

Taking into account that the lifetime of Cr^{2+} ions in ZnSe is ~5μs, we could estimate that the effective Cr→Fe energy transfer rate is faster than 1 μs. Hence, the kinetics and PL experiments demonstrate that the energy transfer rate at RT in Cr-Fe pairs could be faster than the upper level life of Fe^{2+} ions and Cr-Fe energy transfer could be used as a pump mechanism for Fe^{2+} lasers.

3. Discussion

The ground state of the free $Fe^{2+}(3d^6)$ and $Cr^{2+}(3d^4)$ ions is the ^{5}D state with total degeneracy 25. It is split into $^5T_2$ triplet and ^{5}E duplet in the tetrahedral crystal field of II-VI chalcogenides. In the ZnSe crystal field, doublet ^{5}E is the ground state of the iron ions, while $^5T_2$ is the ground state of the chromium ions. The low temperature structure of the emission and absorption bands could be explained by combinations of spin-orbit and dynamic/static Jahn–Teller distortion as well as electron-phonon coupling. Since there is no strong hierarchy over these interactions, the detailed energy structures are still subjects for theoretical interpretation. However, the RT emission spectrum of Cr^{2+} ions and absorption spectrum of Fe^{2+} ions reveal spectral structure which is usually fitted by two Gaussian curves. This structure is usually explained by dynamic Jahn-Teller distortion resulting in splitting of the $^5T_2$ level on $^5\hat{E}$ and $^5\hat{B}_2$ states. It is accompanied by the reduction of T_d symmetry of the TM ion to D_2d symmetry [16]. It is also supported by the additional broad mid-IR absorption band in chromium doped compounds due to the $^5\hat{B}_2 \rightarrow {}^5\hat{E}$ transition (see Fig. 1). The RT absorption at the transition between $^5T_2$ components is ~30 times smaller than at the $^5T_2 \rightarrow {}^5E$ transition in the Cr:ZnSe crystal. The absorption and emission cross-sections of iron and chromium doped II-VI materials were calculated from independent measurements [12]. The absorption cross sections are calculated from the absorption coefficient and concentration of the TM ions, while the spectrum of the emission cross-section is usually estimated from the Füchtbauer–Ladenburg equation [17]:

$$\sigma_{em}(\lambda) = \frac{\lambda^5 c^2}{8\pi c n^2 T_{rad}} \frac{P_w(\lambda)}{\int \lambda P_w(\lambda) d\lambda}, \tag{1}$$

where n is refractive index, c is the speed of light, T_{rad} is radiation lifetime, and $P_W(\lambda)$ is spectral intensity distribution of spontaneous emission. The validity of using of the Füchtbauer–Ladenburg equation for transition metal ion emission bands featuring strong electron phonon coupling and additional energy splitting of laser levels could be tested by relations between emission and absorption oscillator strengths. The latter could be calculated from the cross section spectra using the following equation [18]:

$$f_{if} = (4\pi\varepsilon_0)\frac{mc}{\pi e^2}\int \sigma_{if}(v)dv, \tag{2}$$

where indexes i and f are used for initial and final energy states. The theory predicts the relationship between the emission oscillator strength and the absorption oscillator strength as follows [18]:

$$\frac{f_{em}}{f_{ab}} = \frac{g_l}{g_u}, \tag{3}$$

where g_l and g_u are the degeneracy of lower and upper energy levels. The used optical parameters and calculated values are summarized in Table 2.

It should be noted that the splitting of the $^5T_2$ level by the Jahn–Teller effect is not supposed to change the degeneracy, because in the case of the Fe^{2+} ion, the g_u value should include all energy sub levels contributing to the absorption band. As well as in the case of the Cr^{2+} ion, the g_l value should include all the energy sub levels making contribution to the emission band. As one can see from Table 2 the relationship between emission and absorption oscillator strengths are in a good agreement with theoretical prediction. It indicates that the Füchtbauer–Ladenburg equation is a

Table 2. Summary of spectroscopic properties at $^5T_2 \rightarrow {}^5E$ transition of Cr^{2+} and Fe^{2+} ions in ZnSe crystal (optical bandwidth are measured at full width at half maximum)

Parameter	Cr^{2+}	Fe^{2+}
max σ_{ab}, 10^{-18}cm^2	1.1	0.97
$\Delta\nu_{ab}$, cm^{-1}	1150	1300
f_{ab}	1.5×10^{-3}	1.4×10^{-3}
g_u	10	15
max σ_{em}, 10^{-18}cm^2	1.3	1.1
$\Delta\nu_{em}$, cm^{-1}	1530	605
f_{em}	2.2×10^{-3}	8.1×10^{-4}
g_l	15	10
f_{em}/f_{ab}	1.47	0.59
g_l/g_u	1.5	0.67

good approximation for the emission cross-section calculation in spite of complicated structure of the emission and absorption bands of Cr^{2+} and Fe^{2+} ions in II-VI materials.

The microscopic energy transfer process could be considered using the Förster-Dexter model. According to this model, the energy transfer rate from donor to acceptor can be expressed in terms of the oscillator strength of the D*→D and A→A* transitions (where asterisk indicates the excited state). In the case of the electric dipole-dipole interaction between donor and acceptor separated by a distance R, the energy transfer rate could be calculated from equation [19]:

$$W_{DA}^{dd} \equiv \frac{1}{T_{DA}} = \left(\frac{1}{4\pi\varepsilon_0}\right)^2 \left(\frac{3\pi\hbar e^4}{m^2\omega^2 n^4}\right) \frac{\tilde{f}_D \tilde{f}_A}{R^6} \int g_D(E) g_A(E) dE, \tag{4}$$

where $\tilde{f}_{D,\ A}$ is the oscillator strength of the donor and acceptor transitions corrected using the local field factor $\tilde{f}_{if} = f_{if}\left[n\left(\frac{3}{n^2+2}\right)^2\right]$. The overlap integral contains normalized shape functions for emission ($g_D(E)$) and absorption ($g_A(E)$) transitions of the donor and acceptor, respectively. The energy transfer rates at RT for $(Cr^{2+})^* \rightarrow (Cr^{2+})$, $(Cr^{2+})^* \rightarrow (Fe^{2+})$, and $(Fe^{2+})^* \rightarrow (Fe^{2+})$ processes at different TM concentrations are summarized in Table 1. The minimum distance (R_{min}) used in the calculations was equal to 0.4 nm which corresponds to the distance between TM ions located in the nearest Zn nodes in the ZnSe lattice. The characteristic distance between TM ions for different concentrations (N) could be estimated using the relationship $R_N = \sqrt[3]{1/N}$. As one can see from the Table 1, the energy transfer in Cr-Cr and Fe-Fe pairs could be as fast as ~1 ns, when TM ions are located in the nearest cation positions. However, for a concentration $N = 2\times10^{19}$ cm^{-3} ($R_N \approx 3.7$ nm), the energy transfer time increases to 230 and 850 µs for iron and chromium pairs, correspondingly. In the case of a homogeneous distribution of TM ions, each excited ion has six acceptors at this distance. Therefore the total energy transfer time could be estimated as 38 and 140 µs at RT. In the Cr-Fe pairs with minimum distance between ions, the energy transfer time could be as fast as 320 ps, while at R_N=3.7 nm it estimated to be 33µs. These calculations demonstrate that the energy transfer rate between TM ions could be very fast in the case of small separation between ions. This rate is faster than non-radiative relaxation in Fe^{2+} ions at RT. However, calculated rates for a homogenous distribution of TM ions predicts a smaller rate than measured in the experiments. For example, the energy transfer rate estimated from concentration quenching of Cr^{2+} PL should be of the order of ~1/5µs in the samples with a chromium concentration of ~2×10^{19} cm^{-3} [13]. This difference may result from the non-homogenous distribution of TM ions. In some doped materials, the distortion of the crystal lattice due to dopant results in formation of the aggregate centers even at small concentrations [20].

4. Conclusions

The RT temperature kinetics of the Fe:Cr:ZnSe sample under excitation of chromium at 1560 nm shows that the energy transfer in Fe-Cr centers could be as fast as 290 ns. This rate is close to the non-radiative relaxation rate of Fe^{2+} ions in this host. It is demonstrated that optimization of chromium and iron concentrations in the ZnSe crystal enables an efficient Cr→Fe energy transfer. Therefore, efficient pumping of Cr lasers by the radiation of Er or Tm fiber lasers could be applicable for Fe^{2+} laser systems as well. In addition, Fe:Cr:ZnSe crystal cooling strongly suppresses non-radiative decay of Fe^{2+} ions and provides a better overlap between the absorption band of iron and the emission band of chromium ions. All above indicates, that co-doped Fe:Cr:ZnSe crystals are attractive mid-IR laser media.

Funding

Air Force Office of Scientific Research (AFOSR) (FA9550-13-1-0234); U.S. Department of Energy (DOE) (DE-SC0018378).

Acknowledgments

The authors would like to acknowledge funding support from the AF Office of Scientific Research (Award No. FA9550-13-1-0234) and the Department of Energy (DE-SC0018378).

Disclosures

The work reported here partially involves intellectual property developed at the University of Alabama at Birmingham. This intellectual property has been licensed to the IPG Photonics Corporation. Drs. Fedorov and Mirov declare competing financial interests.

References

1. J. J. Adams, C. Bibeau, R. H. Page, D. M. Krol, L. H. Furu, and S. A. Pane, "4.0-4.5 um lasing of Fe:ZnSe below 180, a new mid-infrared laser material," Opt. Lett. **24**(23), 1720–1722 (1999).
2. J. Kernal, V. V. Fedorov, A. Gallian, S. B. Mirov, and V. V. Badikov, "3.9-4.8 µm gain-switched lasing of Fe:ZnSe at room temperature," Opt. Express **13**(26), 10608–10615 (2005).
3. A. D. Martinez, D. V. Martyshkin, R. P. Camata, V. V. Fedorov, and S. B. Mirov, "Crystal field engineering of transition metal doped II-VI ternary and quaternary semiconductors for mid-IR tunable laser applications," Opt. Mater. Express **5**(9), 2036–2046 (2015).
4. M. E. Doroshenko, H. Jelínková, M. Jelínek, J. Šulc, D. Vyhlídal, N. O. Kovalenko, and I. S. Terzin, "Room temperature Fe^{2+}:$Cd_{1-x}Mn_xTe$ laser generating at 5.4–6 µm," Opt. Lett. **43**(20), 5058–5061 (2018).
5. M. E. Doroshenko, V. V. Osiko, H. Jelínková, M. Jelínek, J. Šulc, M. Němec, D. Vyhlídal, M. Čech, N. O. Kovalenko, and A. S. Gerasimenko, "Spectroscopic and laser properties of bulk iron doped zinc magnesium selenide Fe:ZnMgSe generating at 4.5–5.1 µm," Opt. Express **24**(17), 19824–19834 (2016).
6. J. W. Evans, B. D. Dolasinski, T. R. Harris, J. W. Cleary, and P. A. Berry, "Demonstration and power scaling of an Fe:CdMnTe laser at 5.2 microns," Opt. Mater. Express **7**(3), 860–867 (2017).
7. V. V. Fedorov, S. B. Mirov, A. Gallian, D. V. Badikov, M. P. Frolov, Yu. V. Korostelin, V. I. Kozlovsky, A. I. Landman, Yu. P. Podmar'kov, V. A. Akimov, and A. A. Voronov, "3.77–5.05-mm Tunable Solid-State Lasers Based on Fe^{2+}-Doped ZnSe Crystals Operating at Low and Room Temperatures," IEEE J. Quantum Electron. **42**(9), 907–917 (2006).
8. A. A. Voronov, V. I. Kozlovsky, Yu. V. Korostelin, A. I. Landman, Yu. P. Podmar'kov, Ya. K. Skasyrsky, and M. P. Frolov, "A continuous-wave Fe^{2+}:ZnSe laser," Quantum Electron. **38**(12), 1113–1116 (2008).
9. S. D. Velikanov, V. P. Danilov, N. G. Zakharov, N. N. Il'ichev, S. Yu. Kazantsev, V. P. Kalinushkin, I. G. Kononov, A. S. Nasibov, M. I. Studenikin, P. P. Pashinin, K. N. Firsov, P. V. Shapkin, and V. V. Shchurov, "Fe^{2+}:ZnSe laser pumped by a non-chain electric-discharge HF laser at room temperature," Quantum Electron. **44**(2), 141–144 (2014).
10. N. Myoung, D. V. Martyshkin, V. V. Fedorov, and S. B. Mirov, "Mid-IR lasing of iron–cobalt co-doped ZnS(Se) crystals via Co–Fe energy transfer," J. Lumin. **133**, 257–261 (2013).

Optical Materials EXPRESS

11. J. M. Peppers, D. V. Martyshkin, V. V. Fedorov, and S. B. Mirov, “Spectroscopic characterization and energy transfer process in cobalt and cobalt-iron co-doped ZnSe/ZnS crystals,” Proc. SPIE **8959**, 89591P (2014).
12. S. Mirov, V. Fedorov, D. Martyshkin, I. Moskalev, M. Mirov, and S. Vasilyev, “Progress in Mid-IR Lasers Based on Cr and Fe Doped II-VI Chalcogenides,” IEEE J. Sel. Top. Quantum Electron. **21**(1), 292–310 (2015).
13. A. Burger, K. Chattopadhyay, J.-O. Ndap, X. Ma, S. H. Morgan, C. I. Rablau, C.-H. Su, S. Feth, R. H. Page, K. I. Schaffers, and S. A. Payne, “Preparation conditions of chromium doped ZnSe and their infrared luminescence properties,” J. Cryst. Growth **225**(2-4), 249–256 (2001).
14. U. Hömmerich, I. K. Jones, Ei Ei Nyein, and S. B. Trivedi, “Comparison of the optical properties of diffusion-doped polycrystalline Cr:ZnSe and Cr:CdTe windows,” J. Cryst. Growth **287**(2), 450–453 (2006).
15. N. Myoung, V. V. Fedorov, S. B. Mirov, and L. E. Wenger, “Temperature and concentration quenching of mid-IR photoluminescence in iron doped ZnSe and ZnS laser crystals,” J. Lumin. **132**(3), 600–606 (2012).
16. J. T. Vallin, G. A. Slack, and S. Roberts, “Infrared Absorption in some II-VI compounds with Cr,” Phys. Rev. B **2**(11), 4313–4333 (1970).
17. F. Träger, *Springer Handbook of Lasers and Optics* (Springer, 2007).
18. G. Drake, *Springer Handbook of Atomic, Molecular, and Optical* Physics (Springer, 2006).
19. B. Henderson and G. F. Imbusch, *Optical Spectroscopy of Inorganic Solids* (Oxford University Press, 2006).
20. Yu. V. Orlovskii, V. V. Fedorov, T. T. Basiev, J. Heber, B. Leu, M. Altwein, and S. B. Mirov, “Non radiative relaxation and inhomogeneous splitting of aggregated optical centers in the Nd^{3+} doped CaF_2 and SrF_2 crystals (FLN and decay study),” J. Lumin. **83-84**, 361–366 (1999).